

EFFECT OF THE FLEXIBILITY OF AUTOMOTIVE SUSPENSION COMPONENTS IN MULTIBODY DYNAMICS SIMULATIONS

J.-Y. LIM, W.-J. KANG*, D.-S. KIM and G.-H. KIM

Structural Durability Research Center, Korea Automotive Technology Institute, 74 Yongjeong-ri, Pungse-myeon, Cheonan-si, Chungnam 330-912, Korea

(Received 23 February 2007; Revised 19 October 2007)

ABSTRACT—In this study, the effects of flexible bodies in vehicle suspension components were investigated to enhance the accuracy of multibody dynamic simulation results. Front and rear suspension components were investigated. Sub-frames, a stabilizer bar, a tie rod, a front lower control arm, a front knuckle, and front struts were selected. Reverse engineering techniques were used to construct a virtual vehicle model. Hard points and inertia data of the components were measured with surface scanning equipment. The mechanical characteristics of bushings and dampers were obtained from experiments. Reaction forces calculated from the multibody dynamics simulations were compared with test results at the ball joint of the lower control arm in both time-history and range-pair counting plots. Simulation results showed that the flexibility of the strut component had considerable influence on the lateral reaction force. Among the suspension components, the flexibility of the sub-frame, steering knuckle and upper strut resulted in better correlations with test results while the other flexible bodies could be neglected.

KEY WORDS : Multibody dynamics simulation, Virtual testing laboratory (VTL), Flexibility, Suspension

1. INTRODUCTION

Virtual engineering is one of the powerful design methodologies in the automotive industry because it reduces the cost and period of vehicle development. The multibody dynamics model of a vehicle has much utility in the virtual design process. Although it can be applied to the design of crashworthy structures, ride-handling and durability are the major fields of applications (Dias and Pereira, 2004; Kim *et al.*, 1996; Yi, 2000). The reaction force on each component can be evaluated under various driving conditions and, hence, it is possible to predict the durability of automotive parts at a very early design stage. However, a more rigorous and accurate reaction force should be guaranteed for the durability evaluation than the one for the ride and handling analysis since the amplitude of the load history is very sensitive to the fatigue life of an automotive part; see Ellyn (1997). The multibody dynamics model of a vehicle consists of rigid bodies connected to each other with non-linear force elements and joint constraints that limit the motion of the rigid bodies. The proper mechanical characteristics of the force elements, such as dampers and elastomeric bushings, need to be taken into account in the model. Cho

and Choi (2007) analyzed the ride quality according to the non-linearities of suspension parameters and found the effect of the dynamic viscosity of oil.

Virtual technology in a point of vehicle durability can be divided into two categories: Virtual Testing Laboratory (VTL) and Virtual Proving Ground (VPG). The primary difference between the two is the method for the generation of wheel forces in the vehicle model. The former needs the direct input of wheel forces acquired from driving tests while the latter calculates the wheel forces at the contact interfaces between the tires and road. Although the VTL concept has the disadvantage of measuring or estimating wheel forces, the results are much more reliable than that of the VPG concept, which needs an accurate tire model as well as road surfaces. Mousseau *et al.* (1999) coupled the multibody dynamics model of a vehicle with a finite element tire model by a parallel processing algorithm for the VPG. Figure 1 shows examples of the two methodologies.

For fast computation as well as fast modeling of a virtual vehicle, it is generally useful to consider suspension components as rigid bodies since the elastic deformations of the components are small in comparison with elastomeric components. However, some errors can possibly be imposed on the simulation results if elastic bodies are taken as rigid bodies which have no elastic deformations and vibrations.

*Corresponding author. e-mail: wjkang@katech.re.kr

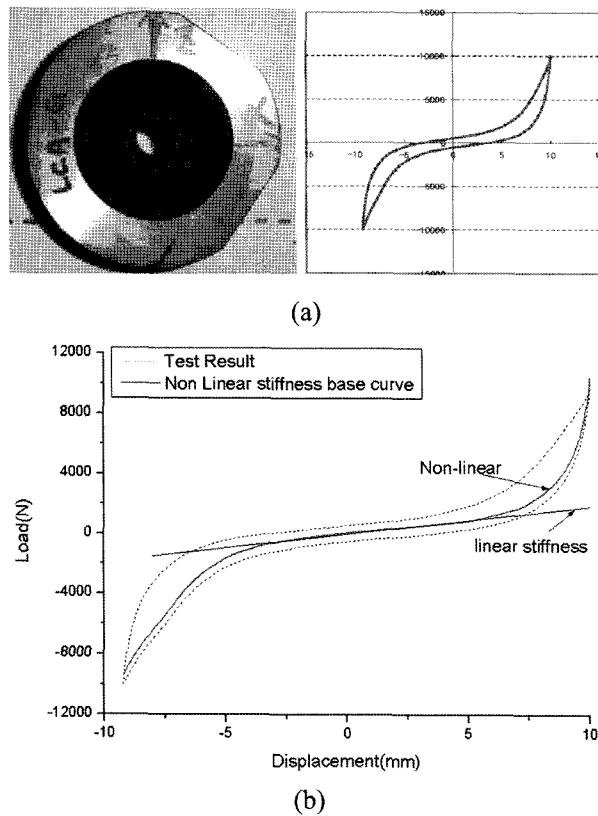


Figure 4. Behavior of a rubber bushing: (a) a lower arm G-bush; (b) non-linear stiffness modeling.

considered. A damper is also an important suspension component that enhances the ride and handling performance by reducing the vibrations of unsprung masses in a vehicle. It behaves according to a nonlinear relation between the reaction force and the relative velocity of the struts. In this study, an optimized numerical model was adopted to describe the damping behavior of each suspension strut instead of a polynomial model. The numerical model can express well the scatter of damping characteristics (Kim *et al.*, 2006).

The connections between parts should be made appropriately to describe the actual kinematic behavior of vehicle components. Between the lower control arms and knuckles, knuckles and tie rods, and lower struts and a stabilizer bar, spherical joints are mounted to constrain the relative translational movements. Fixed joints are mounted between knuckles and lower struts, which eliminate all relative movements between the two parts. Relative movements between lower struts and upper struts are modeled with cylindrical joints. Other than the joints simply getting rid of degrees of freedom, the lower control arms and sub-frames, as well as the car body and sub-frames, are connected with rubber bushing elements. Spring elements mounted between lower struts and upper

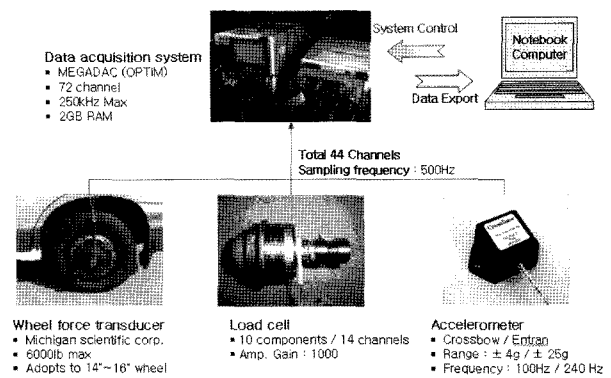


Figure 5. Equipment for driving tests.

struts are modeled with preload conditions such that they are only deformed above permitted values. In the rear suspension, spherical joints between lateral arms and knuckles, lower struts and a stabilizer bar, fixed joints between knuckles and lower struts, and translational joints between lower struts and upper struts are used.

2.2. Wheel Forces and Boundary Conditions

Wheel forces, which were measured by driving tests with wheel force transducers, were imposed on the center of each corresponding wheel. Therefore, a tire model can be excluded from the current multibody dynamics simulations. Figure 5 displays equipment used for the driving tests to acquire wheel forces, body accelerations, and the reaction force of each suspension component. The MEGADAC data acquisition system was used in the measurement of signals from a total of 44 channels. Ten components, including a ball joint of the lower control arm, were monitored by strain gauges and installed in the test vehicle after calibration processes. Linear relations between strain signals and corresponding applied loads were found in all sensorized components. Reaction forces measured during driving tests were compared to the simulation results of the virtual vehicle model.

Boundary conditions were imposed on the model to achieve stable simulation results. It is almost impossible to equilibrate the full vehicle model with the wheel forces measured on the proving ground without exact accordance with masses and mass moment of inertias of sprung masses. Furthermore, it is also difficult to measure the exact inertia property of the sprung mass including a body-in-white. Although a statistical value can be used for the inertia of the sprung mass, it leads to convergence problems with the measured wheel forces. In this study, instead of finding the exact inertia property, vertical accelerations of body-in-white were measured during driving tests with accelerometers attached to the bottom points of B-pillars. The signals were converted into displacements and imposed as boundary conditions

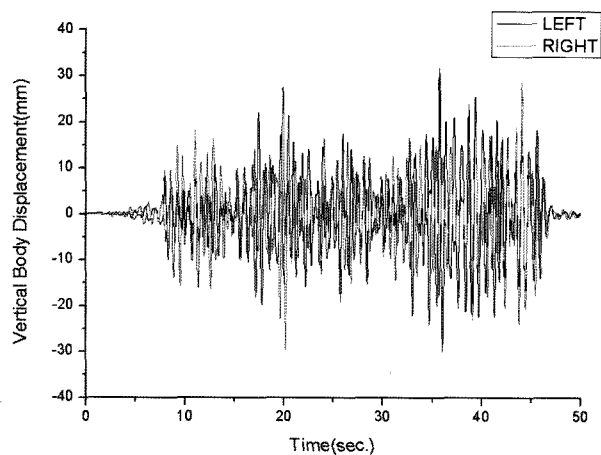


Figure 6. Body displacements to constrain the roll motion measured on a Belgian road at 20 km/h.

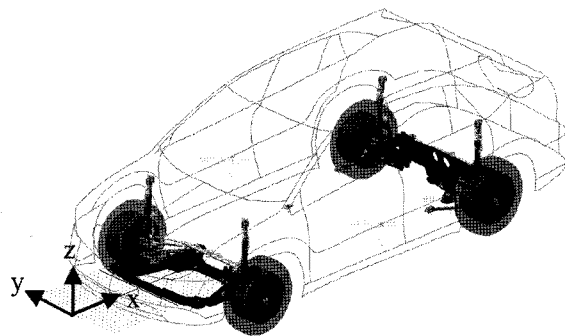


Figure 7. Virtual vehicle model with boundary and loading conditions.

on the vehicle model. Therefore, the roll motion of the sprung mass as well as the vertical translational motion could be determined from the experiment (Figure 6). The pitch and yaw motions were ignored due to their small values compared to the roll motion. The slippage of the vehicle in the longitudinal and lateral directions was also fixed at the center of gravity, which is reasonable considering that the actual values are not large enough.

With these boundary conditions, the mass moment of inertia of the sprung mass is not important and, thus, the total weight and weight of the unsprung masses are the only effective parameter in the simulation, which can be easily measured. Figure 7 shows the full vehicle model constructed in this study with the boundary conditions and the wheel forces as loading conditions.

3. FLEXIBLE BODY ANALYSIS AND RESULTS

3.1. Introduction to the Flexible Body Model

When the wheel forces are applied to the wheel center,

Table 1. First natural frequencies of suspension components.

components	First natural frequency [Hz]
Front Sub-frame	98
Rear Sub-frame	105
Stabilizer bar	55
Tie rod	460
Lower control arm	993
Knuckle	1621
Lower strut	1537
Upper strut	499

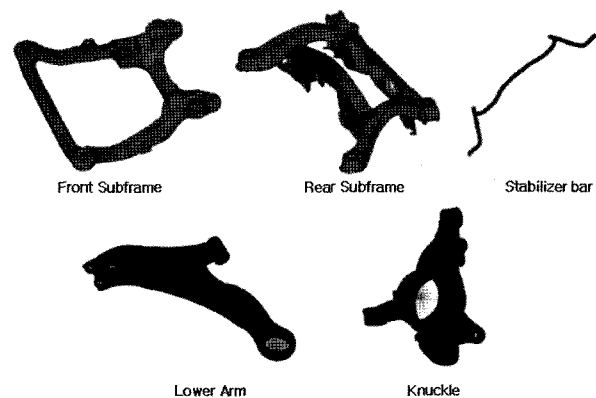


Figure 8. Finite element models of the selected flexible bodies.

suspension components can be elastically deformed with respect to the transferred loads. The deformation is small and, thus, flexibility is neglected in general. As a result, each suspension component is assumed to be a rigid body. However, the assumption of the rigid bodies may have some errors and, hence, the rigid body model can possibly affect the accuracy of simulation results. In this study, the suspension components, such as front and rear sub-frames, front lower control arms, a stabilizer bar, tie rods, knuckles and strut components in the full vehicle model, were investigated to verify the effect of flexibility. Each finite element model of the suspension component is displayed in Figure 8. Normal mode analyses of components were carried out, and the lowest natural frequencies are summarized in Table 1. It should be noted that the lowest natural frequencies of the front and the rear sub-frame, as well as the stabilizer bar, were below about 100 Hz. Power spectral densities of wheel forces are plotted in Figure 9. The major power spectral densities of wheel forces range below about 30 Hz on the standard rough road. However, the power spectral density still has some values up to 100 Hz, even though the value is very small. Thus, it is desirable to investigate resonance effects between wheel forces and suspension com-

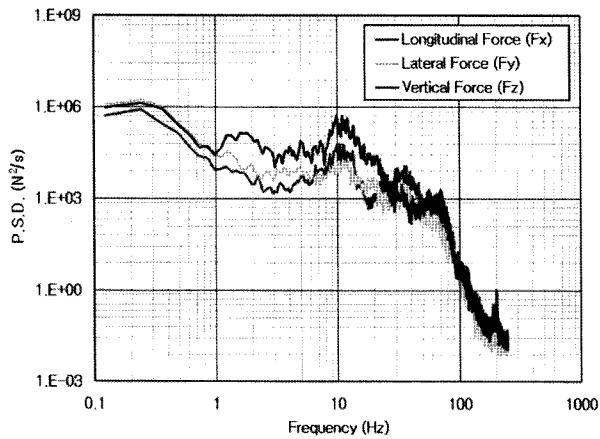


Figure 9. Power spectral densities of wheel forces measured on the standard rough road.

ponents up to this frequency.

In multibody dynamics simulations, nodal coordinates or modal coordinate systems can be applied in order to represent deformations (Geradin and Cardona, 2001). When using the nodal coordinate system, a large memory space and computation time may be required, depending on the size of the finite element model. A natural mode superposition is used in the modal coordinate system to represent elastic deformation (Suh, 2001). It needs relatively little memory space and computation time, but the solution can be affected by the number of the selected natural modes. To obtain better local deformation behavior, static correction modes can be used (Yoo, 1986). In this study, the mode superposition method was used to represent the elastic deformation of each suspension component. In order to incorporate the flexible body effects into the rigid body model, a finite element analysis on each component should be performed in advance to create a modal neutral file (MNF) (see NASTRAN user's manual). Then, the newly created data of MNF replaces the rigid body in the multibody dynamics model,

Table 2. Nomination of the flexible models.

Model	Flexible component
Rigid	Rigid
Flex-1(Flex base)	Front & rear sub-frame
Flex-2	Flex-1+stabilizer bar
Flex-3	Flex-2+tie rod
Flex-4	Flex-3+lower arm
Flex-5	Flex-4+knuckle
Flex-6	Flex-1+lower strut
Flex-7	Flex-1+upper strut
Flex-8	Flex-1+lower/upper strut

which is solved in ADAMS (2006).

Models for parametric studies are nominated in Table 2. A total eight flexible models were simulated with ADAMS. The rigid model has no flexible bodies, and the flexibilities of the front and rear sub-frames were considered in all the other models. The reason to select the sub-frames as major flexible components is that the components have the lowest values of the natural frequency among the considered parts.

3.2. Comparison between the Rigid Body Model and the Flexible Body Model

Reaction forces in the rigid model (Rigid) and the flexible body model (Flex-1 model) were compared with each other together with test results at the ball joint of the front lower control arm. The front and rear sub-frame were modeled as flexible bodies in the Flex-1 model, while all components were assumed to be rigid bodies in the Rigid model. Time histories of the reaction forces at the ball joint are represented in Figure 10. The driving condition is a constant speed of 20 km/h on the cobblestone road. The fluctuation pattern of the test result is simulated well

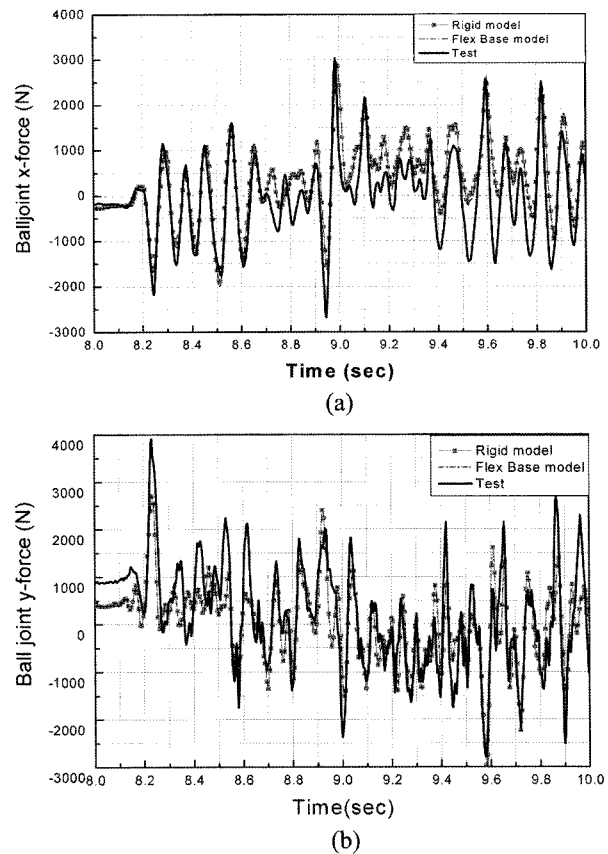


Figure 10. Comparison of the reaction forces at the ball joint on a cobblestone road at 20 km/h: (a) x directional force; (b) y directional force.

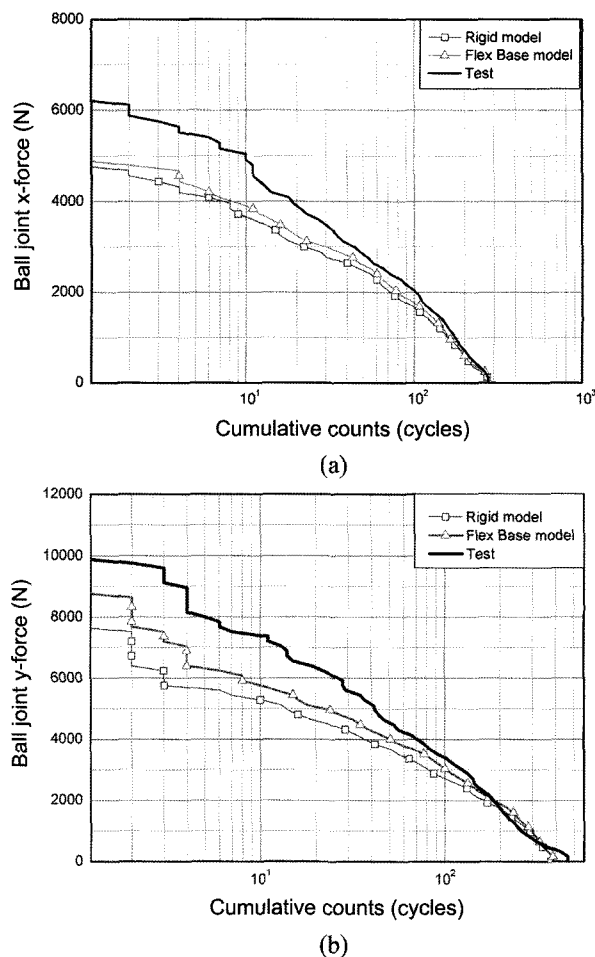


Figure 11. Range pair counts of reaction forces at the ball joint on a cobblestone road at 20 km/h: (a) x directional force; (b) y directional force.

in both models, but the discrepancy between simulation results is not clear in the time history plot. The range-pair cycle counting plot is shown in Figure 11, which has a meaning in the fatigue life evaluation. In this plot, a significant difference can be observed and it will lead to a significant fatigue life deviation.

When the sub-frames are considered as flexible bodies in the multibody dynamics model, the estimated reaction force at the ball joint is bigger than that of the rigid sub-frame case. Although both the simulation results have errors compared with the experiment, it can be noted here that the result is improved by considering the flexible effect of the sub-frames. The difference between the simulation and experiment can be imposed from the assumptions regarding the boundary condition or joint stiffness (neglected in the model) as well as the flexibility of bodies. The rigid body model can be used in the early design state, but it leads to a longer fatigue life compared to the flexible model and test result. Therefore, it is not

acceptable for the safe fatigue design.

3.3. The Effect of Additional Flexible Bodies in the Suspension System

The other flexible components are added up to the Flex-1 model, and the effect of flexibilities are analyzed in this section. The reaction forces at the ball joint of the lower control arm were also investigated; the driving conditions were that of a Belgian road at a speed of 20 km/h. Time histories of the reaction forces are compared in Figure 12. Significant differences in magnitudes and phases between simulation models are not observed in the x directional reaction forces. As shown in the range-pair plot in Figure 13(a), remarkable differences cannot be found either. This feature is almost similar in the y directional reaction forces if the strut members are not modeled as flexible bodies. However, the flexible strut model has an effect on the reaction forces in the y direction as shown in Figure 12(b) and 13(b). It can be caused from the characteristic of the McPherson strut, such that the lateral force can be generated due to the spring deformation.

The Flex-6 model produces the highest value of the ball joint reaction forces, and the Flex-7 model shows

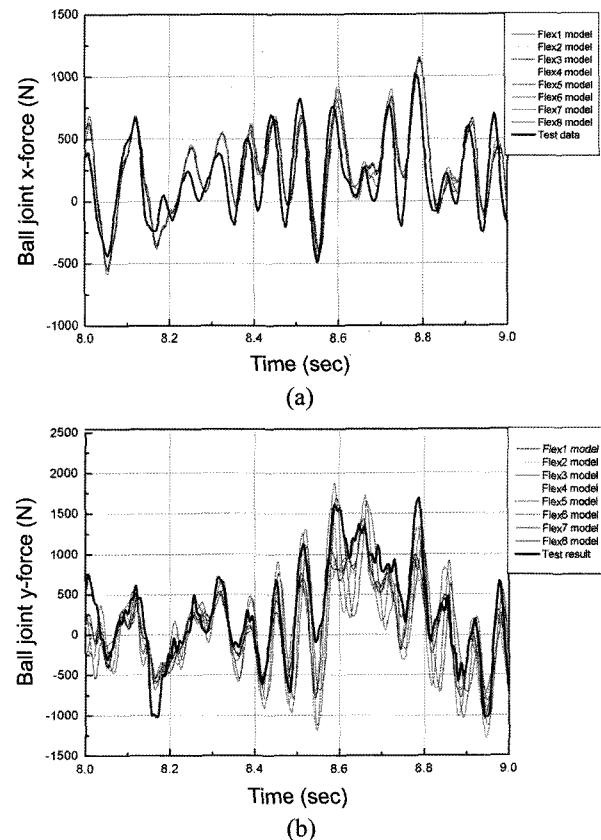
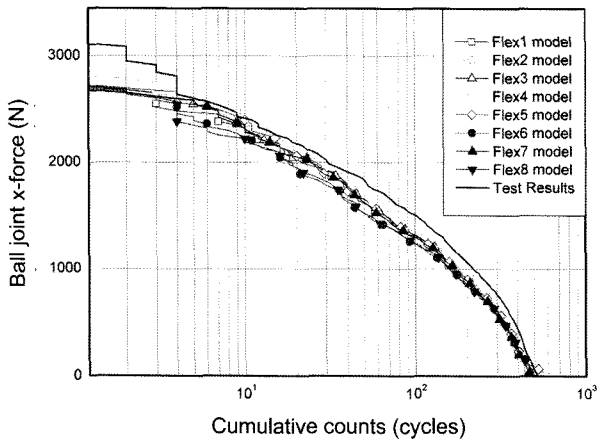
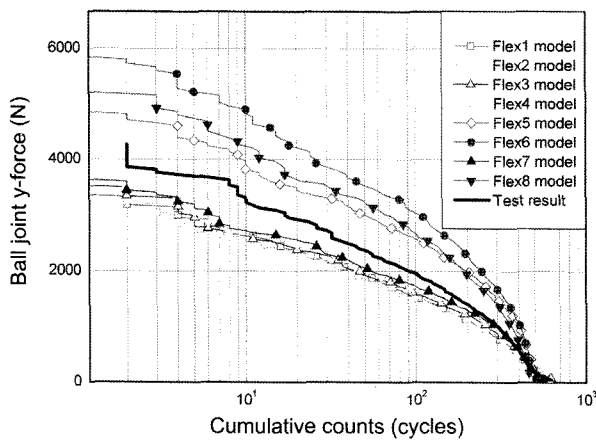


Figure 12. Comparison of reaction forces at the ball joint on a Belgian road at 20 km/h: (a) x directional force; (b) y directional force.



(a)



(b)

Figure 13. Range pair counts of reaction forces at the ball joint on a Belgian road at 20 km/h: (a) x directional force; (b) y directional force.

slightly improved results from the models whose strut members are rigid. The results of the Flex-8 model are in between those from the Flex-6 and the Flex-7 models. This feature of the flexibility of the strut member is also discovered in the cobblestone driving analysis, as shown in Figure 14. The closest case to the test result is the Flex-7 model, which considers the sub-frames and upper struts as flexible bodies. With regard to how conservative the fatigue design is, the results of the Flex-5 through Flex-8 models are acceptable in the design for the vehicle durability except for the Flex-6 model. The Flex-6 model results in the highest values, which are quite different from the test results. Since the flexible model shows the enhanced results of the load amplitudes, especially in the high amplitude region, the accumulated damages calculated from the loads will be much more improved from the point of view of a fatigue analysis.

The Flex-3 and Flex-4 models do not show much deviation, but the computation time increases to over two

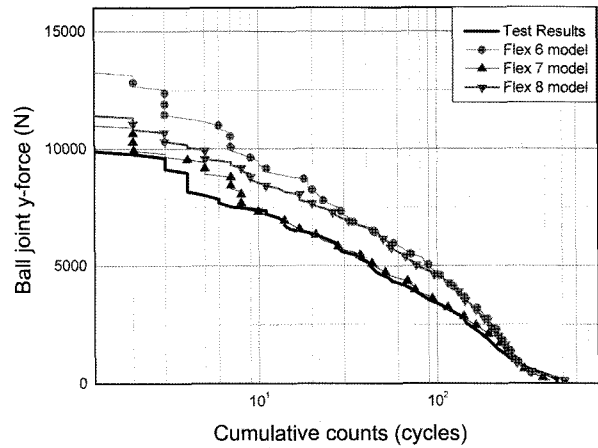


Figure 14. Range pair counts of reaction forces at the ball joint of the front lower control arm measured on a cobblestone road at 20 km/h.

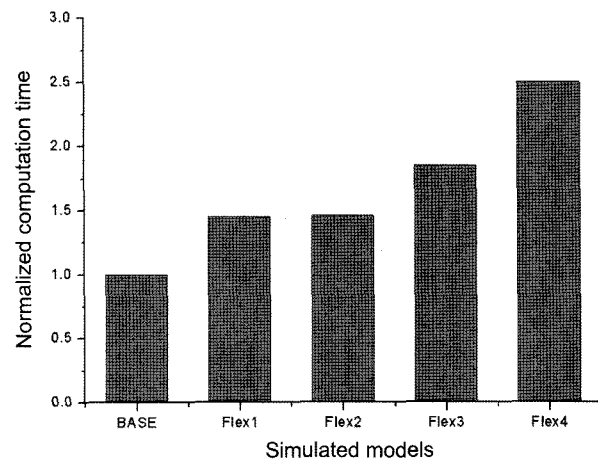


Figure 15. Normalized computation time.

times that of the rigid body model. The first natural frequencies of the suspension components are generally far higher than the frequencies of wheel forces or reaction forces on components. This means that the components are stiff enough not to allow severe flexible effects. Nevertheless, to get accurate multibody dynamics simulation results for the improved fatigue analysis, it is recommended that the flexibilities of the sub-frames, steering knuckles, and upper struts be considered in the virtual vehicle model. Other components will increase the computation cost without any significant improvements.

4. CONCLUSION

In this study, the effects of the flexibility of suspension components in a virtual vehicle model were investigated in order to acquire accurate reaction forces on the components. The components, such as sub-frames, a stabilizer

bar, lower control arms, tie rods, knuckles and strut members, were investigated. The results of reaction forces were analyzed in load-time history and range-pair counting plots, which are meaningful for the fatigue life analysis. The Flex-7 model, which incorporates the sub-frames and upper struts as flexible bodies, predicted the most accurate solution compared with the test result. With regard to safe fatigue design, it is recommended that the flexibilities of the sub-frames, steering knuckles, and upper struts be considered in the virtual vehicle model. Other components will increase the computation cost without significant improvements.

ACKNOWLEDGEMENT—The developed work reported herein was funded by the Ministry of Commerce, Industry and Energy of Korea. The authors wish to gratefully appreciate their support during this work.

REFERENCES

- ADAMS (2006). *User's Manual*. MSC. Los Angeles.
- Cho, S. J. and Choi, Y. S. (2007). Estimation of ride quality of a passenger car with nonlinear suspension. *Int. J. Automotive Technology* **8**, **1**, 103–109.
- Dias, J. P. and Pereira, M. S. (2004). Optimization methods for crashworthiness design using multibody models. *Computers & Structures*, **82**, 1371–1380.
- Ellyin, F. (1997). *Fatigue Damage, Crack Growth and Life Prediction*. 1st edn. Chapman & Hall. London.
- Geradin, M. and Cardona, A. (2001). *Flexible Multibody Dynamics*. John Wiley & Sons. New York.
- Kim, G. H., Kang, W. J., Kim, D. S., Ko, W. H. and Lim, J. Y. (2006). The durability performance evaluation of automotive components in the virtual testing laboratory. *Trans. Korean Society Automotive Engineers* **1**, **3**, 68–74.
- Kim, K. S., Yoo, W. S. Lee, K. H. and Kim, K. T. (1996). Effect of chassis flexibility on ride quality. *Trans. Korean Society Automotive Engineers* **4**, **2**, 127–136.
- Moon, I. D. and Oh, C. Y. (2003). Development of a computer model of a large-scale truck considering the frame as a flexible body. *Trans. Korean Society Automotive Engineers* **11**, **6**, 197–204.
- Mousseau, C. W., Laursen, T. A., Lidberg, M. and Taylor, R. L. (1999). Vehicle dynamics simulations with coupled multibody and finite element models. *Finite Elements in Analysis and Design*, **31**, 295–315.
- MSC/NASTRAN (1993). *User's Guide*. 68. Los Angeles.
- Pan, W. and Haug, E. J. (1999). Flexible multibody dynamic simulation using optimal lumped inertia matrices. *Comput. Methods Appl. Mech. Engrg.*, **173**, 189–200.
- Simeon, B. (2006). On Lagrange multipliers in flexible Multibody dynamics. *Comput. Methods Appl. Mech. Engrg.*, **195**, 6993–7005.
- Suh, K. H. (2001). Dynamic stress analysis of a vehicle frame by flexible multibody dynamics simulation. *SAE Paper No.* 2001-01-0032.
- Yi, T. Y. (2000). Vehicle dynamic simulations based on flexible and rigid multibody models. *SAE Paper No.* 2000-01-0114.
- Yoo, Y. S. and Haug, E. J. (1986). Dynamics of flexible mechanical systems using vibration and static correction modes. *ASME, J. Mechanisms, Transmissions and Automation in Design*, **108**, 315–322.